Graph Signal Processing for Directed Graphs based on the Hermitian Laplacian

Satoshi Furutani[1] (✉), Toshiki Shibahara[1], Mitsuaki Akiyama[1],
Kunio Hato[1], and Masaki Aida[2]

[1] NTT Secure Platform Laboratories, Tokyo, Japan,
{satoshi.furutani.ek, toshiki.shibahara.de, kunio.hato.gm}@hco.ntt.co.jp,
akiyama@ieee.org,
[2] Tokyo Metropolitan University, Tokyo, Japan
aida@tmu.ac.jp

Abstract. Graph signal processing is a useful tool for representing, analyzing, and processing the signal lying on a graph, and has attracted attention in several fields including data mining and machine learning. A key to construct the graph signal processing is the graph Fourier transform, which is defined by using eigenvectors of the graph Laplacian of an undirected graph. The orthonormality of eigenvectors gives the graph Fourier transform algebraically desirable properties, and thus the graph signal processing for undirected graphs has been well developed. However, since eigenvectors of the graph Laplacian of a directed graph are generally not orthonormal, it is difficult to simply extend the graph signal processing to directed graphs. In this paper, we present a general framework for extending the graph signal processing to directed graphs. To this end, we introduce the Hermitian Laplacian which is a complex matrix obtained from an extension of the graph Laplacian. The Hermitian Laplacian is defined so as to preserve the edge directionality and Hermitian property and enables the graph signal processing to be straightforwardly extended to directed graphs. Furthermore, the Hermitian Laplacian guarantees some desirable properties, such as non-negative real eigenvalues and the unitarity of the Fourier transform. Finally, experimental results for representation learning and signal denoising of/on directed graphs show the effectiveness of our framework.

Keywords: Graph signal processing · Graph Laplacian · Directed graph.

1 Introduction

Graph signal processing has attracted attention in several fields since it is useful for representing, analyzing, and processing the *graph signal*, which is the signal defined on the nodes of a graph. Graph signal processing aims to extend the classical signal processing for signals on a Euclidean structure, e.g., time series and image signals, to signals on any graphs (i.e., both undirected and directed graphs). The basic concepts of graph signal processing have already been introduced, such as graph filtering [18,19,23], graph sampling [4,32] and graph-based

transforms [13, 24, 29]. Along with theoretical development, graph signal processing has facilitated advances in data mining, such as community mining [33], shape classification [16], feature learning [35], and representation learning [8]. Furthermore, it is a fundamental theory for generalizing machine learning algorithms for data with an underlying Euclidean or grid-like structure to graph structures, e.g., semi-supervised learning [1, 11] and deep neural networks [3, 6].

Fourier transform of graph signal, called *graph Fourier transform*, plays a key role in constructing the graph signal processing. The basic approach to define the graph Fourier transform is based on eigenvectors of the graph Laplacian [13, 29]. This approach applies to undirected graphs and constructs the Fourier basis as the eigenvector of the graph Laplacian. Because of its orthonormality, the resulting Fourier transform is unitary, and thus the inner product is preserved. Furthermore, since this transform is considered as the natural extension of classical Fourier transform, the Fourier basis is easy to interpret. Specifically, the Fourier basis corresponding to low frequency varies slowly, whereas that corresponding to high frequency varies intensively. However, since eigenvectors of the graph Laplacian of a directed graph are generally not orthonormal, we cannot straightforwardly extend the graph Fourier transform to directed graphs.

The alternative approach to define the graph Fourier transform is based on the Jordan decomposition of the adjacency matrix [23, 24]. This approach constructs the Fourier basis by using generalized eigenvectors of the adjacency matrix. This is motivated by the fact that the adjacency matrix of a directed ring graph can be regarded as the shift operator for discrete signals [21]; shift operator is the basis of all shift-invariant linear filtering. Since any square matrices can be decomposed as Jordan form, this approach is applicable to both undirected and directed graphs. However, it has some unsolved critical issues. First, since the Fourier basis based on the Jordan decomposition is not orthonormal, the resulting transform is not unitary. Second, the Fourier basis corresponding to low frequency does not necessarily vary slowly and vice-versa [31]. Third, eigenvalues of the adjacency matrix of a directed graph will take complex values. The complex eigenvalues lead to a large error in the approximated filter responses [22]. Finally, the numerical computation of the Jordan decomposition often incurs numerical instabilities even for medium-sized matrices [12].

A few unique approaches have recently been proposed to extend the graph Fourier transform to directed graphs. Sevi *et al.* [26, 27] proposed a framework for constructing the harmonic analysis (i.e., Fourier and wavelet transform) on directed graphs based on the Dirichlet energy of eigenfunctions of a random walk operator. This approach constructs the Fourier basis by using the eigenfunction of the random walk Laplacian [5] of a directed graph. However, this approach is applicable only to strongly connected directed graphs and does not guarantee the orthonormality of the Fourier basis. Another approach is to construct the Fourier basis by solving the non-convex optimization problems under some constraints. Sardellitti *et al.* [25] proposed a method for constructing the Fourier basis as the solution of the minimization problem of Lovász extension of the graph cut under the orthonormality constraints. Lovász extension is a lossless convex relaxation

of the graph cut and is read as a smoothness measure of a graph signal. Then, Shafipour *et al.* [28] designed the Fourier basis as the solution of the non-convex orthonormality constrained optimization problems such that frequencies have a desirable property, i.e., frequencies associated with the Fourier bases are evenly spread over the entire frequency domain. Although these methods can construct Fourier bases that have desirable properties, the solutions (Fourier bases) may fall into a local minimum and can vary each time depending on the solving method and/or initial conditions. Moreover, the Fourier bases do not completely preserve the information about an underlying graph structure. Namely, it is difficult to reconstruct the graph structure from Fourier bases and frequencies.

In this paper, we present a general framework for extending the graph signal processing to directed graphs based on the Hermitian Laplacian. The Hermitian Laplacian is defined so as to preserve both the Hermitian property and edge directionality by encoding the edge direction into the argument (phase) in the complex plane. Thanks to the Hermitian property, we can always choose eigenvectors of a Hermitian Laplacian as orthonormal bases. This orthonormality enables the basic concepts of the graph signal processing for undirected graphs to be straightforwardly generalized to that for directed graphs. Furthermore, the Hermitian property guarantees some desirable properties for constructing the graph signal processing, such as non-negative real eigenvalues and the unitarity of the Fourier transform. Finally, we provide experimental results for representation learning and signal denoising of/on directed graphs as application examples of our framework.

2   Preliminaries

2.1   Graph Laplacian and Graph Signals

Let $G = (V, E)$ be an undirected graph without self-loops and multiple edges, where V is the set of N nodes and $E \subset V \times V$ is the set of edges in G. The adjacency matrix $\boldsymbol{A} = [A_{ij}] \in \mathbb{R}^{N \times N}$ is defined as $A_{ij} = w_{ij}$ if $(i, j) \in E$ and $A_{ij} = 0$ otherwise. Here w_{ij} is the real positive weight of edge (i, j), and $w_{ij} = w_{ji}$ in an undirected graph. The degree of each node is $d_i := \sum_{j=1}^{N} w_{ij}$ and the degree matrix is defined as $\boldsymbol{D} := \mathrm{diag}(d_1, \ldots, d_N)$. The graph Laplacian is defined as $\boldsymbol{L} := \boldsymbol{D} - \boldsymbol{A}$.

For connected graphs, $\boldsymbol{L}$ is a non-negative definite matrix and its minimum eigenvalue is 0. Therefore we sort its eigenvalues in ascending order as $0 = \lambda_0 < \lambda_1 \leq \cdots \leq \lambda_{N-1}$, and we choose the orthonormal eigenvector $\boldsymbol{v}_\mu$ associated with eigenvalue λ_μ such that $\langle \boldsymbol{v}_\mu, \boldsymbol{v}_\nu \rangle = \delta_{\mu\nu}$, where $\delta_{\mu\nu}$ is Kronecker's delta. Then, since $\boldsymbol{L}$ of an undirected graph G is real symmetric, $\boldsymbol{L}$ can be decomposed as $\boldsymbol{L} = \boldsymbol{V}\boldsymbol{\Lambda}\boldsymbol{V}^*$, where $\boldsymbol{V} := (\boldsymbol{v}_0, \ldots, \boldsymbol{v}_{N-1})$ is the orthonormal matrix, $\boldsymbol{\Lambda} = \mathrm{diag}(\lambda_0, \ldots, \lambda_{N-1})$ is the diagonal matrix, and * is the adjoint (conjugate transpose). Note that, for undirected graphs, $\boldsymbol{V}^* = \boldsymbol{V}^T$ since $\boldsymbol{V}$ is real.

The graph signal $\boldsymbol{f} : V \to \mathbb{R}^N$ can be represented as a N dimensional vector whose i-th entry $f(i)$ is the signal value at node $i \in V$.

2.2   Graph Signal Processing

In this subsection, we briefly introduce the Laplacian-based graph signal processing [13, 29] through comparison with classical signal processing.

Graph Fourier transform. The classical Fourier transform is defined by the inner product of signal $f(t)$ with the Fourier basis $e^{\mathrm{i}\omega t}$ as

$$\hat{f}(\omega) := \langle f, e^{\mathrm{i}\omega t} \rangle = \int_{\mathbb{R}} f(t) \, e^{-\mathrm{i}\omega t} \, \mathrm{d}t.$$

This means Fourier transform is the expansion of a function f by the Fourier basis that is the eigenfunction of the one-dimensional Laplace operator; $-\triangle e^{\mathrm{i}\omega t} = -\frac{\partial^2}{\partial t^2} e^{\mathrm{i}\omega t} = \omega^2 e^{\mathrm{i}\omega t}$.

Analogously, for undirected graphs, the graph Fourier transform of graph signal $\boldsymbol{f} \in \mathbb{R}^N$ is defined by the eigenvectors of graph Laplacian $\boldsymbol{L}$ as

$$\hat{f}(\lambda_\mu) := \langle \boldsymbol{f}, \boldsymbol{v}_\mu \rangle = \sum_{i=1}^{N} f(i) \, v_\mu^*(i), \tag{1}$$

$$\hat{\boldsymbol{f}} := \boldsymbol{V}^* \boldsymbol{f}, \tag{2}$$

and inverse graph Fourier transform is defined as $\boldsymbol{f} := \boldsymbol{V}\hat{\boldsymbol{f}}$.

In classical Fourier analysis, the eigenvalue ω^2 can be intepreted as frequency: the eigenfunction $e^{\mathrm{i}\omega t}$ varies slowly for small ω but intensively for large ω. In the graph setting, the eigenvalues and eigenvectors of graph Laplacian also act identically. For connected graphs, the eigenvector $\boldsymbol{v}_0$ associated with zero eigenvalue λ_0 is constant; $v_0(i) = 1/\sqrt{N}$ for all i. Then, the eigenvector associated with small eigenvalue varies slowly across the graph. In other words, if two nodes are connected, the corresponding entries of the eigenvector have similar values. This fact is confirmed by the following equation:

$$\lambda_\mu = \boldsymbol{v}_\mu^T \boldsymbol{L} \boldsymbol{v}_\mu = \sum_{(i,j)\in E} w_{ij} \left(v_\mu(i) - v_\mu(j) \right)^2, \tag{3}$$

which is instantly derived from $\boldsymbol{\Lambda} = \boldsymbol{V}^* \boldsymbol{L} \boldsymbol{V}$. Hereinafter, the property that small and large eigenvalues correspond to low and high frequencies, respectivery, is referred to as *frequency ordering*.

Spectral graph filtering. In classical signal processing, filtering is the process that removes some unwanted components from an input signal f_{in}. Let h be the filter in the time domain. The filtering is defined by the convolution of f_{in} and h as

$$f_{\mathrm{out}}(t) := \int_{-\infty}^{\infty} f_{\mathrm{in}}(\tau) \, h(t - \tau) \, \mathrm{d}\tau. \tag{4}$$

Taking the Fourier transform of (4), we derive

$$\hat{f}_{\text{out}}(\omega) = \hat{f}_{\text{in}}(\omega)\,\hat{h}(\omega), \tag{5}$$

so-called *convolution theorem*.

We can generalize (5) to define spectral graph filtering as

$$\hat{f}_{\text{out}}(\lambda_\mu) = \hat{f}_{\text{in}}(\lambda_\mu)\,\hat{h}(\lambda_\mu), \tag{6}$$

or, equivalently, we have

$$f_{\text{out}}(i) = \sum_{\mu=0}^{N-1} \hat{f}_{\text{in}}(\lambda_\mu)\,\hat{h}(\lambda_\mu)\,v_\mu(i). \tag{7}$$

We can also write (7) by matrix form as

$$\boldsymbol{f}_{\text{out}} := \boldsymbol{V}\hat{\boldsymbol{H}}\boldsymbol{V}^*\boldsymbol{f}_{\text{in}}, \tag{8}$$

where $\hat{\boldsymbol{H}} := \text{diag}(\hat{h}(\lambda_0), \dots, \hat{h}(\lambda_{N-1}))$ and $\hat{h}(\lambda)$ is the filter kernel function defined on $[0, \lambda_{N-1}]$.

Spectral graph wavelet transform. Spectral graph wavelet transform is defined by using the Fourier basis previously defined. The construction of wavelets is based on band-pass or low-pass filters in the frequency domain, generated by modulating a unique filter kernel $\hat{g}(s\,\cdot)$ defined on $[0, \lambda_{N-1}]$. The wavelet at scale $s(>0)$ and node i is defined as

$$\boldsymbol{\psi}_{s,i} := \boldsymbol{V}\hat{\boldsymbol{G}}_s\boldsymbol{V}^*\boldsymbol{\delta}_i, \tag{9}$$

where $\hat{\boldsymbol{G}}_s := \text{diag}(\hat{g}(s\lambda_0), \dots, \hat{g}(s\lambda_{N-1}))$ and $\boldsymbol{\delta}_i$ is the vector whose i-th entry is 1 and others are 0. Then, given any signal $\boldsymbol{f} \in \mathbb{R}^N$, the wavelet coefficient is defined as

$$W_f(s,i) := \langle \boldsymbol{f}, \boldsymbol{\psi}_{s,i} \rangle = \boldsymbol{\psi}_{s,i}^*\,\boldsymbol{f}.$$

3   Graph Signal Processing for Directed Graphs based on the Hermitian Laplacian

Obviously, if the graph Laplacian of a directed graph has orthonormal eigenvectors, we can naturally extend the graph signal processing to directed graphs. However, since the graph Laplacian of a directed graph is asymmetric, its eigenvectors are generally not orthonormal. To overcome this non-orthonormality issue, we introduce the Hermitian Laplacian which is a complex matrix obtained from an extension of the graph Laplacian. The Hermitian Laplacian is defined so as to preserve the edge directionality and Hermitian property and enables the graph signal processing to be straightforwardly extended to directed graphs.

3.1   Hermitian Laplacian on Directed Graphs

Hermitian Laplacian. Here we consider a directed graph $\mathcal{G} = (\mathcal{V}, \mathcal{E})$ where $\mathcal{V}$ is the set of N nodes and $\mathcal{E}$ is the set of directed edges such that for each $i, j \in \mathcal{V}$ ordered tuple $(i, j) \in \mathcal{E}$ assigns a directed edge from node i to j. The weighted adjacency matrix $\boldsymbol{A} = [\mathcal{A}_{ij}] \in \mathbb{R}^{N \times N}$ is defined as $\mathcal{A}_{ij} = w_{ij}$ if $(i, j) \in \mathcal{E}$ and $\mathcal{A}_{ij} = 0$ otherwise. Note that, for a given directed graph, we can uniquely determine the corresponding undirected graph $\mathcal{G}^{(s)} = (\mathcal{V}, \mathcal{E}^{(s)})$ by ignoring the directionality of edges. The (symmetrized) adjacency matrix $\boldsymbol{A}^{(s)} = [w_{ij}^{(s)}]$ of $\mathcal{G}^{(s)}$ is defined as $w_{ij}^{(s)} := \frac{1}{2}(w_{ij} + w_{ji})$.

As is well known, a Hermitian matrix $\boldsymbol{H} \in \mathbb{C}^{N \times N}$ is a complex square matrix that is equal to its own adjoint matrix; $\boldsymbol{H} = \boldsymbol{H}^*$. The significant properties of Hermitian matrices are as follows:

- The sum of any two Hermitian matrices is Hermitian.
- All eigenvalues of a Hermitian matrix are real.
- A Hermitian matrix has linearly independent eigenvectors. Moreover, N eigenvectors can always be chosen as orthonormal bases of $\mathbb{C}^N$.
- Any Hermitian matrix $\boldsymbol{H}$ can be decomposed as $\boldsymbol{H} = \boldsymbol{U}\boldsymbol{\Lambda}\boldsymbol{U}^*$ where $\boldsymbol{U}$ is a unitary matrix whose columns are its eigenvectors, and $\boldsymbol{\Lambda}$ is a diagonal matrix of its eigenvalues.

The above properties of a Hermitian matrix, especially the orthonormality of its eigenvectors, motivate us to define the graph Laplacian of a directed graph as a Hermitian matrix. For this purpose, we consider the edge directionality and node connectivity separately, and encode the edge direction into the argument (phase) in the complex plane.

Let us define the function $\gamma : \mathcal{V} \times \mathcal{V} \to U(1)$ such that

$$\gamma(i, j) = \overline{\gamma(j, i)}, \tag{10}$$

where $U(1)$ is the unitary group of degree 1. One of the simplest expressions of γ is

$$\gamma_q(i, j) := \gamma(i, j; q) = e^{\mathrm{i}2\pi q(w_{ij} - w_{ji})}, \tag{11}$$

where $q \in [0, 1)$ is a rotation parameter. As shown in Fig. 1, $\gamma_q(i, j)$ encodes the direction of (i, j) into the phase in the complex plane.

By using (11), the Hermitian Laplacian is defined as

$$\boldsymbol{\mathcal{L}}_q := \boldsymbol{D} - \boldsymbol{\Gamma}_q \odot \boldsymbol{A}^{(s)}, \tag{12}$$

where $\boldsymbol{D}$ is the degree matrix of $\mathcal{G}^{(s)}$, $\boldsymbol{\Gamma}_q$ is a Hermitian matrix whose (i, j) component is $\gamma_q(i, j)$, and $\odot$ is Hadamar product. Since $\boldsymbol{\Gamma}_q \odot \boldsymbol{A}^{(s)}$ is Hermitian, $\boldsymbol{\mathcal{L}}_q$ is Hermitian. In addition, the degree normalized version of $\boldsymbol{\mathcal{L}}_q$, which is given by $\boldsymbol{\mathcal{N}}_q := \boldsymbol{D}^{-1/2}\boldsymbol{\mathcal{L}}_q\boldsymbol{D}^{-1/2}$, is also Hermitian.

In the context of quantum physics, the Hermitian Laplacian can be interpreted as the operator that describes the phenomenology of a free charged particle on a graph, which is subject to the action of a magnetic field. Therefore,
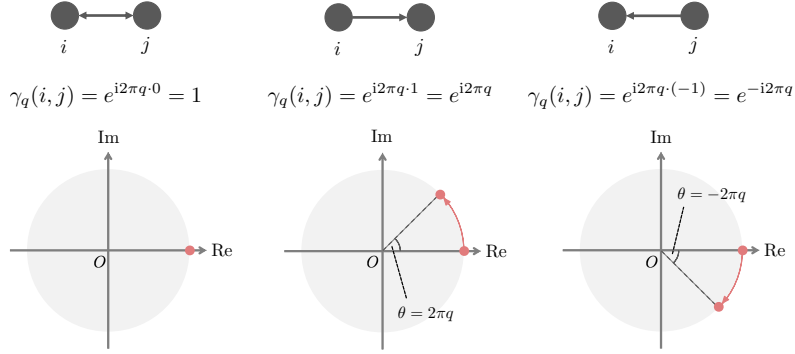
$$\gamma_q(i,j) = e^{i2\pi q \cdot 0} = 1 \qquad \gamma_q(i,j) = e^{i2\pi q \cdot 1} = e^{i2\pi q} \qquad \gamma_q(i,j) = e^{i2\pi q \cdot (-1)} = e^{-i2\pi q}$$

Fig. 1. γ encodes the edge direction into the phase in the complex plane

it is called *magnetic Laplacian* [2, 7, 14, 34]. Due to this physical context, the parameter q is named *electric charge*. Some applications of the magnetic Laplacian for directed graphs have been proposed, e.g., visualization [9], community detection [10], and characterization [17].

Spectral properties. Let us look at the spectral properties of the Hermitian Laplacian via relationship with the ordinary graph Laplacian. We denote the eigenvalues of the Hermitian Laplacian $\boldsymbol{\mathcal{L}}_q$ in ascending order as $\lambda_0' \leq \cdots \leq \lambda_{N-1}'$, and choose the eigenvector $\boldsymbol{u}_\mu$ associated with λ_μ' as the orthonormal eigenbasis. As it is clear from (11), if $\mathcal{G}$ is undirected or $q = 0$, the Hermitian Laplacian $\boldsymbol{\mathcal{L}}_q$ is equivalent to an ordinary graph Laplacian $\boldsymbol{L}$ since $\gamma_q(i,j) = 1$ for all $(i,j) \in \mathcal{V} \times \mathcal{V}$. Thus, for small q, the spectrum of the Hermitian Laplacian is expected to be analogous to the spectrum of the graph Laplacian, such as the presence of a zero eigenvalue and frequency ordering.

We first consider Kato's inequality [15] for the Hermitian Laplacian to look at the relationship between the smallest eigenvalue of $\boldsymbol{\mathcal{L}}_q$ and $\boldsymbol{L}$.

Proposition 1. *For any signal $\boldsymbol{f} \in \mathbb{C}^N$, the following inequality holds:*

$$\langle |\boldsymbol{f}|, \boldsymbol{L}|\boldsymbol{f}| \rangle \leq \mathrm{Re}\left[\langle \boldsymbol{f}, \boldsymbol{\mathcal{L}}_q \boldsymbol{f} \rangle\right], \tag{13}$$

where $|\boldsymbol{f}|$ is the real vector whose i-th entry is $|f(i)|$.

Proof. By explicit calculation, we obtain

$$\langle |\boldsymbol{f}|, \boldsymbol{L}|\boldsymbol{f}| \rangle - \mathrm{Re}\left[\langle \boldsymbol{f}, \boldsymbol{\mathcal{L}}_q \boldsymbol{f} \rangle\right]$$

$$= \sum_{i,j=1}^{N} w_{ij}^{(s)} \left(|f(i)|^2 - |f(i)||f(j)|\right) - \mathrm{Re}\left[\sum_{i,j=1}^{N} w_{ij}^{(s)} \left(|f(i)|^2 - \gamma_q(i,j)\,\overline{f(i)}\,f(j)\right)\right]$$

$$= \sum_{i,j=1}^{N} w_{ij}^{(s)} \left(\mathrm{Re}\left[\gamma_q(i,j)\,\overline{f(i)}\,f(j)\right] - |f(i)||f(j)|\right) \leq 0,$$

since $\operatorname{Re}\left[\overline{f(i)}\,f(j)\right] \leq |f(i)||f(j)|$ and $|\gamma_q(i,j)| = 1$ for any q. $\square$

Recall that the smallest eigenvalue of the Hermitian Laplacian $\boldsymbol{\mathcal{L}}_q$ is computed as

$$\lambda'_0 = \inf\left\{ \frac{\langle \boldsymbol{f}, \boldsymbol{\mathcal{L}}_q \boldsymbol{f}\rangle}{\langle \boldsymbol{f}, \boldsymbol{f}\rangle} \mid \langle \boldsymbol{f}, \boldsymbol{f}\rangle \neq 0 \right\},$$

we have the immediate corollary of Proposition 1.

Corollary 1. *For any q, the smallest eigenvalue of $\boldsymbol{L}$ and $\boldsymbol{\mathcal{L}}_q$ have the following relationship:*

$$0 = \lambda_0 \leq \lambda'_0. \tag{14}$$

This suggests that the Hermitian Laplacian has non-negative real eigenvalues.

Next, to measure the smoothness of eigenvectors of $\boldsymbol{\mathcal{L}}_q$, we introduce the total variation. We define the total variation of signal $\boldsymbol{f} \in \mathbb{C}^N$ on a graph $\mathcal{G}$ as

$$\mathrm{TV}(\boldsymbol{f}) := \sum_{(i,j)\in\mathcal{E}} |f(i) - f(j)|^2. \tag{15}$$

As it is clear from (15), $\mathrm{TV}(\boldsymbol{f})$ is small (large) if any two adjacent signals on $\mathcal{G}$ take similar (dissimilar) values, respectively. Therefore, we find that (15) measures the smoothness of signals over a graph. Figure 2 shows an example of eigenvalues and total variations of eigenvectors of the Hermitian Laplacian $\boldsymbol{\mathcal{L}}_q$ on a random directed graph with 50 nodes. From this figure, one can find that $\boldsymbol{\mathcal{L}}_q$ satisfies the frequency ordering and has a nearly zero eigenvalue for small q but not for large q because of a larger contribution from the imaginary part.

3.2   Graph Signal Processing for Directed Graphs

In this subsection, we explain the graph signal processing for directed graphs based on the Hermitian Laplacian. As described in Sect. 2.2, the graph Laplacian of an undirected graph has a zero eigenvalue and satisfies the frequency ordering. These properties are useful for understanding the physical meaning of the Fourier basis. Therefore, for extending graph signal processing to directed graphs, the Hermitian Laplacian should also satisfy these properties. For this purpose, we first describe the condition of the rotation parameter q so that $\boldsymbol{\mathcal{L}}_q$ satisfies these properties. Then, we define the graph Fourier transform and some other concepts of graph signal processing on directed graphs.

Selection of q. The choice of the rotation parameter q influences the graph Fourier transform. However, there is not an established method to select it. We here propose an expedient method to select q for graph signal processing. Let ϵ be the tolerance of the smallest eigenvalue λ'_0 of the Hermitian Laplacian $\boldsymbol{\mathcal{L}}_q$ $(q > 0)$ of an unweighted directed graph $\mathcal{G}$, that is $0 \leq \lambda'_0 \leq \epsilon$. Then, let us denote the
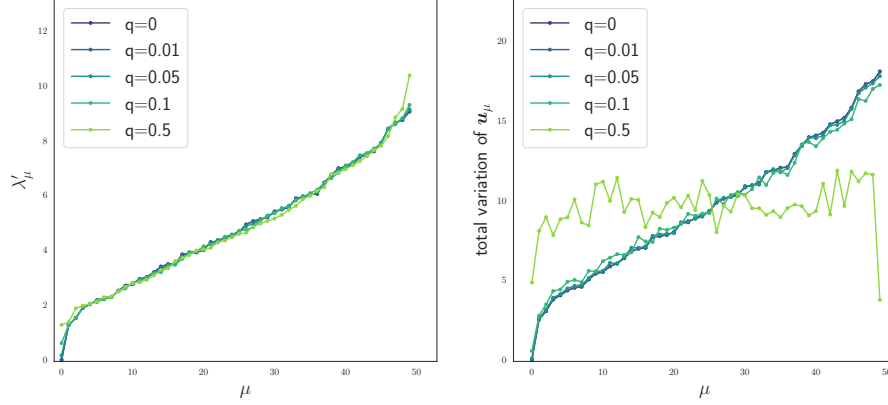
Fig. 2. Spectral properties of the Hermitian Laplacian of a random directed graph with 50 nodes; average degree $\langle d \rangle = 5$.

eigenvalue and associated eigenvector of the symmetrized Laplacian $\boldsymbol{L}^{(s)}$ ($= \mathcal{L}_0$) of $\mathcal{G}^{(s)}$ as $\lambda_\mu^{(s)}$ and $\boldsymbol{u}_\mu^{(s)}$, respectively. According to eigenvalue perturbation theory [20], for small q, the eigenvalue λ'_μ of $\mathcal{L}_q$ is approximated as

$$\lambda'_\mu \simeq \lambda_\mu^{(s)} + \langle \boldsymbol{u}_\mu^{(s)}, \boldsymbol{\Delta}_q \boldsymbol{u}_\mu^{(s)} \rangle, \tag{16}$$

where $\boldsymbol{\Delta}_q := \mathcal{L}_q - \boldsymbol{L}^{(s)}$. Thus, the smallest eigenvalue of $\mathcal{L}_q$ is

$$\lambda'_0 \simeq \lambda_0^{(s)} + \langle \boldsymbol{u}_0^{(s)}, \boldsymbol{\Delta}_q \boldsymbol{u}_0^{(s)} \rangle = \frac{1}{N} \sum_{(i,j) \in \mathcal{E}^{(s)}} (\boldsymbol{\Delta}_q)_{ij},$$

$$\leq \frac{1}{2N} |\mathcal{E}| (2 - e^{\mathrm{i}2\pi q} - e^{-\mathrm{i}2\pi q}) = \frac{\langle d \rangle}{2} (1 - \cos(2\pi q)),$$

where $\langle d \rangle = \frac{2|\mathcal{E}|}{N}$ is the average in- or out-degree of $\mathcal{G}$. Therefore, by solving the inequality $\lambda'_0 \leq \frac{\langle d \rangle}{2}(1 - \cos(2\pi q)) \leq \epsilon$, we obtain

$$0 \leq q \leq \frac{\cos^{-1}(1 - 2\epsilon/\langle d \rangle)}{2\pi}. \tag{17}$$

Thus, one can choose q depending only on the average degree $\langle d \rangle$ and the tolerance ϵ of the smallest eigenvalue λ'_0.

Graph Fourier transform on directed graphs. Next, we define the graph Fourier transform on directed graphs. Since $\mathcal{L}_q$ is Hermitian, the Hermitian Laplacian can be represented as $\mathcal{L}_q = \boldsymbol{U}\boldsymbol{\Lambda}'\boldsymbol{U}^*$, where $\boldsymbol{U} = (\boldsymbol{u}_0, \ldots, \boldsymbol{u}_{N-1})$ and $\boldsymbol{\Lambda}' = \mathrm{diag}(\lambda'_0, \ldots, \lambda'_{N-1})$. The graph Fourier transform of the graph signal

$\boldsymbol{f} \in \mathbb{R}^N$ on a directed graph can be straightforwardly defined by replacing $\boldsymbol{V}$ of (2) with $\boldsymbol{U}$ as follows:

$$\hat{\boldsymbol{f}} := \boldsymbol{U}^* \boldsymbol{f}, \tag{18}$$

where $\hat{\boldsymbol{f}} \in \mathbb{C}^N$ is generally a complex valued vector. Note that, since $\boldsymbol{U}$ is orthonormal, this definition (18) of graph Fourier transform holds *Parseval's identity*. In other words, for any graph signal $\boldsymbol{f} \in \mathbb{R}^N$, its Fourier transform $\hat{\boldsymbol{f}}$ preserves the inner product; $\langle \boldsymbol{f}, \boldsymbol{f} \rangle = \langle \hat{\boldsymbol{f}}, \hat{\boldsymbol{f}} \rangle$. This means the Fourier transform is unitary.

In the same way, we can easily extend the concepts of the Laplacian-based graph signal processing on undirected graphs to directed graphs. For example, the spectral graph filtering and spectral graph wavelet on a directed graph are respectively defined as

$$\boldsymbol{f}_{\text{out}} := \boldsymbol{U} \hat{\boldsymbol{H}} \boldsymbol{U}^* \boldsymbol{f}_{\text{in}}, \tag{19}$$

and

$$\boldsymbol{\psi}_{s,i} := \boldsymbol{U} \hat{\boldsymbol{G}}_s \boldsymbol{U}^* \boldsymbol{\delta}_i. \tag{20}$$

4   Experiments and Results

In this section, we provide experimental results of representation learning and signal denoising of/on a directed graph as application examples of graph signal processing based on the Hermitian Laplacian. In each experiment, we set the parameter q of Hermitian Laplacian $\boldsymbol{\mathcal{L}}_q$ to $q = 0.02$; our results are not sensitive to small changes in q.

4.1   Representation Learning for Synthetic Graph

We first consider the representation learning of a synthetic directed graph. GraphWave [8] is the representation learning method using the graph signal processing. The embedding function of GraphWave is designed such that structurally similar nodes are embedded close together by leveraging diffusion patterns of each node. We provide an overview of GraphWave below.

For a given graph Laplacian $\boldsymbol{L} = \boldsymbol{V} \boldsymbol{\Lambda} \boldsymbol{V}^T$ of an undirected graph, we here denote the spectral graph wavelet at scale s and node i as $\boldsymbol{\psi}_i(s)$ and its j-th entry as $\psi_{ij}(s)$. If the filter kernel $\hat{g}(s\lambda)$ is heat kernel $\hat{g}(s\lambda) = e^{-s\lambda}$, one can find that the wavelet $\boldsymbol{\psi}_i(s)$ is equal to the solution of the diffusion equation $\frac{\mathrm{d}}{\mathrm{d}s}\boldsymbol{\psi}(s) = -\boldsymbol{L}\boldsymbol{\psi}(s)$ with the initial value $\boldsymbol{\psi}(0) = \boldsymbol{\delta}_i$, since

$$\boldsymbol{\psi}_i(s) = \boldsymbol{V} \hat{\boldsymbol{G}}_s \boldsymbol{V}^T \boldsymbol{\delta}_i = \boldsymbol{V} e^{-s\boldsymbol{\Lambda}} \boldsymbol{V}^T \boldsymbol{\delta}_i, = e^{-s\boldsymbol{V}\boldsymbol{\Lambda}\boldsymbol{V}^T} \boldsymbol{\delta}_i = e^{-s\boldsymbol{L}} \boldsymbol{\delta}_i. \tag{21}$$

Given the embedding parameters, $t \in \{t_1, \ldots, t_d\}$ and $s \in \{s_1, \ldots, s_m\}$, the embedding function $\chi_i : V \to \mathbb{R}^{2dm}$ is defined as follows:

$$\chi_i = [\text{Re}(\phi_i(s,t)), \ \text{Im}(\phi_i(s,t))]_{t \in \{t_1, \ldots, t_d\}, \, s \in \{s_1, \ldots, s_m\}}, \tag{22}$$

where $\phi_i(s,t) := \frac{1}{N}\sum_{j=1}^{N} e^{\mathrm{i}t\,\psi_{ij}(s)}$ is the characteristic function that completely characterizes behavior and properties of the probability distribution. If two nodes are structurally similar within their local graph topology, these diffusion patterns are similar. Therefore, these characteristic functions are also similar, and thus structurally similar nodes are embedded close together. Note that, since eigenvectors of the digraph Laplacian $\boldsymbol{\mathcal{L}} := \boldsymbol{\mathcal{D}} - \boldsymbol{\mathcal{A}}$ are not orthonormal, GraphWave is generally not applicable to directed graphs. However, if the filter kernel is a heat kernel, GraphWave can be made applicable to directed graphs by replacing $\boldsymbol{L}$ of (21) with $\boldsymbol{\mathcal{L}}$, that is $\boldsymbol{\psi}_i(s) = e^{-s\boldsymbol{\mathcal{L}}}\boldsymbol{\delta}_i$.

We evaluate the effectiveness of our framework based on the embedding results by GraphWave for the synthetic directed graph shown in Fig. 3. We set the filter kernel to $\hat{g}(s\lambda) = e^{-s\lambda}$. For comparison, we calculate the embeddings in three ways:

(a) GraphWave based on the symmetrized Laplacian $\boldsymbol{L}^{(s)}$, i.e., ignoring the edge directionality. In this setting, we can directly apply GraphWave to learn embedding.
(b) GraphWave based on the digraph Laplacian $\boldsymbol{\mathcal{L}}$. Since we now assume the heat kernel, we can apply GraphWave to the directed graph as previously mentioned.
(c) GraphWave based on the Hermitian Laplacian $\boldsymbol{\mathcal{L}}_q$, i.e., calculating the wavelet by (20).

To make our evaluation fair, we use the same parameters for each experiment; $s \in \{2.0, 2.1, \ldots, 20.0\}$ and $t \in \{1, 2, \ldots, 10\}$.

Figure 4 shows the results of two-dimensional principal component analysis (PCA) projection of the $\mathbb{R}^{2dm}$ dimensional vector calculated by GraphWave. First, Fig. 4(a) shows that red and blue nodes with the same depth are embedded into the same point without distinction because edge directionality is ignored. Then, Fig. 4(b) reveals that although the edge directionality is considered, sink nodes (nodes with zero out-degree) are embedded into the same point. Specifically, node 13 and nodes 14–17, which are not structurally similar, are embedded into the same point. This is because the characteristic function $\phi_k(s,t)$ is equal for each sink node k, since $\forall s\,\boldsymbol{\psi}_k(s) = \boldsymbol{\psi}_k(0) = \boldsymbol{\delta}_k$. Finally, Fig. 4(c) shows the GraphWave based on the Hermitian Laplacian succeeds at learning embedding while considering edge directionality and distinction of sink nodes. Specifically, our framework can distinguish not only red and blue nodes with same depth but also sink nodes (i.e., node 13 and nodes 14–17).

4.2   Signal Denoising for Graph of Contiguous United States

Next we consider the signal denoising on a directed graph. In this experiment, we use the directed graph that represents the contiguous United States, excluding Alaska and Hawaii which are not connected by land with the other states. A directed edge between states is assigned based on latitudes; from lower to higher. Then, we consider the average annual temperature of each state as the graph
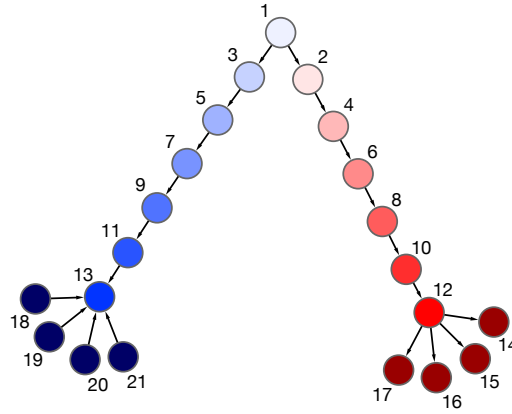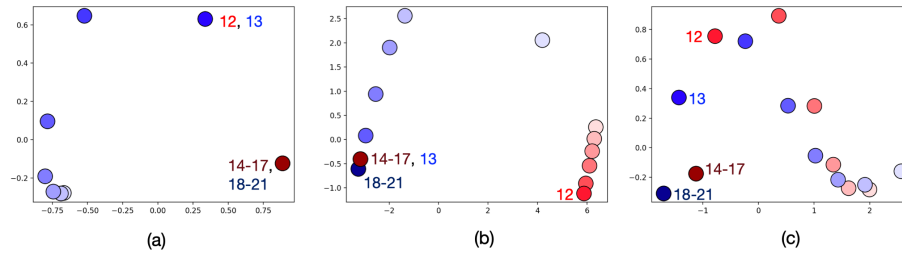
Fig. 3. Synthetic graph.

Fig. 4. Two-dimensional PCA projection of embedding as learned by GraphWave based on the symmetrized Laplacian (a), digraph Laplacian (b) and Hermitian Laplacian (c).

signal[1]. In general, the states closer to the equator, i.e., with lower latitude, have higher average temperatures. Thus, assigning directed edges based on state latitudes may be justified to capture the temperature flow. The same settings were used in [28]. Figure 5 shows the temperature signals over the directed contiguous US graph.

To verify the effectiveness of the graph signal processing based on the Hermitian Laplacian, we conduct an experiment to recover original temperature signals from noisy measurements on both the undirected and directed contiguous US graph. Noisy measurements are generated as $g := f + \eta$, where f is the original signals and η is the noise vector whose each entry $\eta(i)$ independently follows the Gaussian distribution with the mean $\mu = 0$ and standard deviation $\sigma = 10$.

---

[1] Latitude and temperature data are respectively obtained from following web sites: https://inkplant.com/code/state-latitudes-longitudes and
https://www.currentresults.com/Weather/US/average-annual-state-temperatures.php

Then, we use a low-pass filter kernel

$$\hat{h}(\lambda) = \frac{1}{1 + c\lambda},$$

where $c\,(>0)$ is the parameter of this kernel [29]. The recovered (denoised) signal $\tilde{\boldsymbol{f}}$ can be calculated as

$$\tilde{\boldsymbol{f}} = \boldsymbol{U}\hat{\boldsymbol{H}}\boldsymbol{U}^*\boldsymbol{g}, \tag{24}$$

where $\hat{\boldsymbol{H}} := \mathrm{diag}(\hat{h}(\lambda_0), \ldots, \hat{h}(\lambda_{N-1}))$. In this experiment, we set the kernel parameter to $c = 2$. Note that although we here use (23) as low-pass filter kernel, one can choose the other filter kernel, such as [30].

Figure 6 shows an example of the original, noisy and denoised temperature signals on the undirected and directed contiguous US graph. Here, Fig. 6(f) illustrates the real part of each signal, $\mathrm{Re}[\tilde{f}(i)]$, since the denoised signals calculated by (24) are generally complex values. From Fig. 6, one can find that the denoised signals on the undirected graph are comparatively smooth in the entire graph, whereas those on the directed graph are comparatively uneven.

To quantitatively evaluate the denoising performance, we consider the denoising error of each state i, which is calculated as $e(i) := |\mathrm{Re}[\tilde{f}(i)] - f(i)|$. Figure 7 shows the average denoising error $\langle e(i)\rangle$ of each state i over the 100 simulations of independent noise. This figure suggests that the denoising performance in the directed case is equal to or slightly superior to that in the undirected case; especially the signal of peripheral nodes, i.e., the nodes with low or high latitudes, such as FL, TX, LA, MN, MT and ND. In the undirected graph, each denoised signal is simply averaged over its adjacent node signals without considering the edge directionality. This leads denoised signals to be smooth in the entire graph. Therefore, the denoising error will be low in the region where the original signals are smooth but high in the region where they are not. On the other hand, in the directed graph, each denoised signal is averaged over its adjacent node signals while considering the edge directionality. Therefore, it seems that denoised signals capture the temperature flow of original signals without excessive smoothing.

5   Conclusions and Future Work

We have presented a general framework for extending graph signal processing to directed graphs based on the Hermitian Laplacian. The Hermitian Laplacian on a directed graph is defined so as to preserve both the Hermitian property and edge directionality by encoding the edge direction into the phase in the complex plane. The Hermitian property enables the graph signal processing to be straightforwardly generalized to directed graphs and guarantees some desirable properties, such as the non-negative real eigenvalues and the unitarity of the Fourier transform. Based on the Hermitian Laplacian, we have extended the basic concepts of the Laplacian-based graph signal processing on undirected graphs (e.g.,
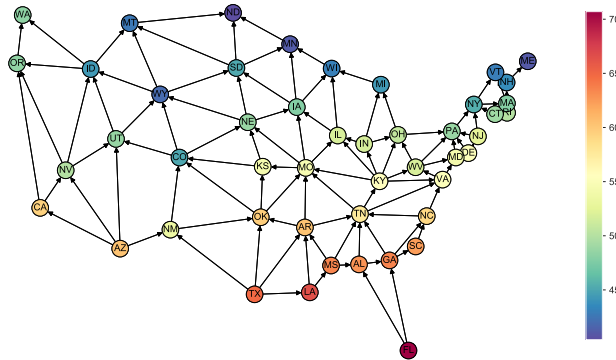
Fig. 5. Graph signal of the average temperature in Fahrenheit for the directed contiguous US.

graph Fourier transform, spectral graph filtering, and spectral graph wavelet) to directed graphs. Finally, we have shown the effectiveness of our framework through two experiments; representation learning and signal denoising of/on a directed graph. Future work includes theoretically analyzing spectral properties of Hermitian Laplacians (e.g., relation between the rotation parameter q and its eigenvectors), evaluating our framework by larger and complex graphs, and developing other applications of our framework.

References

1. Anis, A., El Gamal, A., Avestimehr, S., Ortega, A.: Asymptotic justification of bandlimited interpolation of graph signals for semi-supervised learning. In: 2015 IEEE International Conference on Acoustics, Speech and Signal Processing (ICASSP). pp. 5461–5465. IEEE (2015)
2. Berkolaiko, G.: Nodal count of graph eigenfunctions via magnetic perturbation. Analysis & PDE **6**(5), 1213–1233 (2013)
3. Bronstein, M.M., Bruna, J., LeCun, Y., Szlam, A., Vandergheynst, P.: Geometric deep learning: going beyond Euclidean data. IEEE Signal Processing Magazine **34**(4), 18–42 (2017)
4. Chen, S., Varma, R., Sandryhaila, A., Kovačević, J.: Discrete signal processing on graphs: Sampling theory. IEEE Transactions on Signal Processing **63**(24), 6510–6523 (2015)
5. Chung, F.: Laplacians and the cheeger inequality for directed graphs. Annals of Combinatorics **9**(1), 1–19 (2005)
6. Defferrard, M., Bresson, X., Vandergheynst, P.: Convolutional neural networks on graphs with fast localized spectral filtering. In: Advances in Neural Information Processing Systems. pp. 3844–3852 (2016)
7. Dodziuk, J., Mathai, V.: Kato's inequality and asymptotic spectral properties for discrete magnetic Laplacians. Contemp. Math **398**, 69–81 (2006)
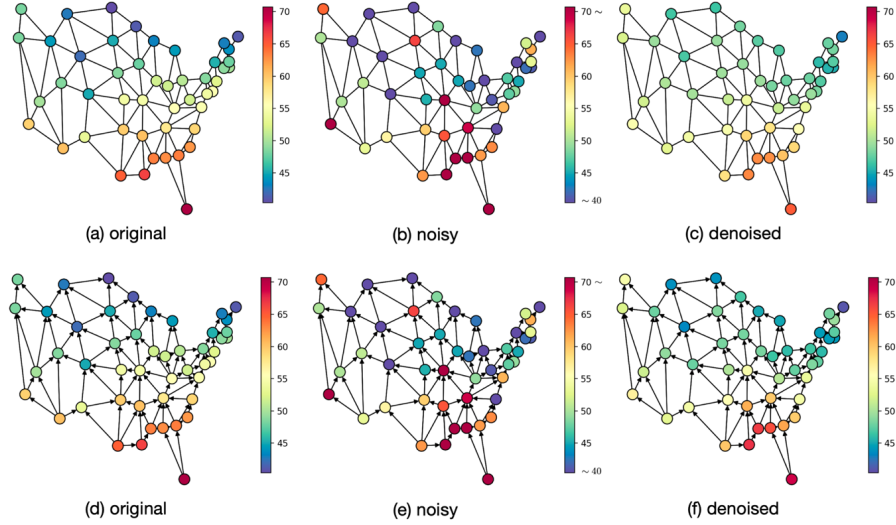
Fig. 6. Original, noisy and denoised temperature signals on undirected (upper panel) and directed (lower panel) contiguous US graph. To equalize colorbar scales for each panel, we set lower limit to $\min_i(f(i)) = 40.4$ and upper limit to $\max_i(f(i)) = 70.7$ in (b) and (e).

8. Donnat, C., Zitnik, M., Hallac, D., Leskovec, J.: Spectral graph wavelets for structural role similarity in networks. arXiv preprint arXiv:1710.10321 (2017)
9. Fanuel, M., Alaíz, C.M., Fernández, Á., Suykens, J.A.: Magnetic eigenmaps for the visualization of directed networks. Applied and Computational Harmonic Analysis **44**(1), 189–199 (2018)
10. Fanuel, M., Alaíz, C.M., Suykens, J.A.: Magnetic eigenmaps for community detection in directed networks. Physical Review E **95**(2), 022302 (2017)
11. Gadde, A., Anis, A., Ortega, A.: Active semi-supervised learning using sampling theory for graph signals. In: ACM SIGKDD international conference on Knowledge discovery and data mining. pp. 492–501 (2014)
12. Golub, G.H., Wilkinson, J.H.: Ill-conditioned eigensystems and the computation of the Jordan canonical form. SIAM review **18**(4), 578–619 (1976)
13. Hammond, D.K., Vandergheynst, P., Gribonval, R.: Wavelets on graphs via spectral graph theory. Applied and Computational Harmonic Analysis **30**(2), 129–150 (2011)
14. Higuchi, Y., Shirai, T.: A remark on the spectrum of magnetic Laplacian on a graph. Yokohama Mathematical Journal **47** (1999)
15. Kato, T.: Schrödinger operators with singular potentials. Israel Journal of Mathematics **13**(1-2), 135–148 (1972)
16. Masoumi, M., Hamza, A.B.: Shape classification using spectral graph wavelets. Applied Intelligence **47**(4), 1256–1269 (2017)
17. Messias, B., Costa, L.d.F.: Characterization and space embedding of directed graphs trough magnetic Laplacians. arXiv preprint arXiv:1812.02160 (2018)
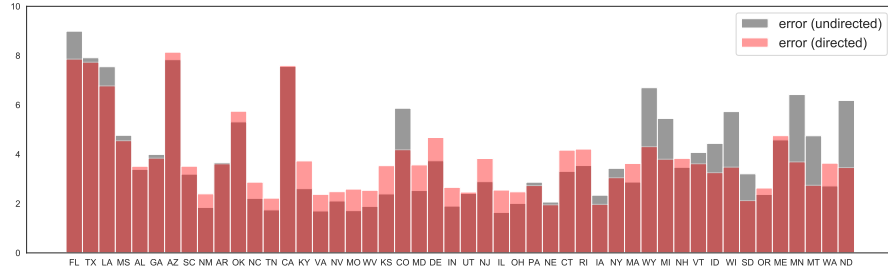
Fig. 7. Semi-transparent bar charts of average denoising error of each state over 100 simulations (in ascending order of state latitudes). The averages of $\langle e(i) \rangle$ in the directed and undirected cases are 3.7719 and 3.8723, respectively.

18. Narang, S.K., Ortega, A.: Perfect reconstruction two-channel wavelet filter banks for graph structured data. IEEE Transactions on Signal Processing **60**(6), 2786–2799 (2012)

19. Narang, S.K., Ortega, A.: Compact support biorthogonal wavelet filterbanks for arbitrary undirected graphs. IEEE transactions on signal processing **61**(19), 4673–4685 (2013)

20. Ngo, K.V.: An approach of eigenvalue perturbation theory. Applied Numerical Analysis & Computational Mathematics **2**(1), 108–125 (2005)

21. Puschel, M., Moura, J.M.: Algebraic signal processing theory: Foundation and 1-D time. IEEE Transactions on Signal Processing **56**(8), 3572–3585 (2008)

22. Sakiyama, A., Namiki, T., Tanaka, Y.: Design of polynomial approximated filters for signals on directed graphs. In: 2017 IEEE Global Conference on Signal and Information Processing (GlobalSIP). pp. 633–637. IEEE (2017)

23. Sandryhaila, A., Moura, J.M.: Discrete signal processing on graphs. IEEE transactions on signal processing **61**(7), 1644–1656 (2013)

24. Sandryhaila, A., Moura, J.M.: Discrete signal processing on graphs: Frequency analysis. IEEE Transactions on Signal Processing **62**(12), 3042–3054 (2014)

25. Sardellitti, S., Barbarossa, S., Di Lorenzo, P.: On the graph Fourier transform for directed graphs. IEEE Journal of Selected Topics in Signal Processing **11**(6), 796–811 (2017)

26. Sevi, H., Rilling, G., Borgnat, P.: Multiresolution analysis of functions on directed networks. In: Wavelets and Sparsity XVII. vol. 10394, p. 103941Q. International Society for Optics and Photonics (2017)

27. Sevi, H., Rilling, G., Borgnat, P.: Harmonic analysis on directed graphs and applications: from Fourier analysis to wavelets. arXiv preprint arXiv:1811.11636 (2018)

28. Shafipour, R., Khodabakhsh, A., Mateos, G., Nikolova, E.: A directed graph Fourier transform with spread frequency components. arXiv preprint arXiv:1804.03000 (2018)

29. Shuman, D.I., Narang, S.K., Frossard, P., Ortega, A., Vandergheynst, P.: The emerging field of signal processing on graphs: Extending high-dimensional data analysis to networks and other irregular domains. IEEE Signal Processing Magazine **30**(3), 83–98 (2013)

30. Shuman, D.I., Ricaud, B., Vandergheynst, P.: Vertex-frequency analysis on graphs. Applied and Computational Harmonic Analysis **40**(2), 260–291 (2016)
31. Singh, R., Chakraborty, A., Manoj, B.: Graph fourier transform based on directed Laplacian. In: 2016 International Conference on Signal Processing and Communications (SPCOM). pp. 1–5. IEEE (2016)
32. Tanaka, Y.: Spectral domain sampling of graph signals. IEEE Transactions on Signal Processing **66**(14), 3752–3767 (2018)
33. Tremblay, N., Borgnat, P.: Graph wavelets for multiscale community mining. IEEE Transactions on Signal Processing **62**(20), 5227–5239 (2014)
34. Colin de Verdière, Y.: Magnetic interpretation of the nodal defect on graphs. Analysis & PDE **6**(5), 1235–1242 (2013)
35. Verma, S., Zhang, Z.L.: Hunt for the unique, stable, sparse and fast feature learning on graphs. In: Advances in Neural Information Processing Systems. pp. 88–98 (2017)